Coral records of central tropical Pacific radiocarbon variability during the last millennium

Laura K. Zaunbrecher,[1,2] Kim M. Cobb,[1] J. Warren Beck,[3] Christopher D. Charles,[4] Ellen R. M. Druffel,[5] Richard G. Fairbanks,[6] Sheila Griffin,[5] and Hussein R. Sayani[1]

Received 12 May 2009; revised 18 May 2010; accepted 7 June 2010; published 10 November 2010.

[1] The relationship between decadal to centennial changes in ocean circulation and climate is difficult to discern using the sparse and discontinuous instrumental record of climate and, as such, represents a large uncertainty in coupled ocean-atmosphere general circulation models. We present new modern and fossil coral radiocarbon ($\Delta^{14}C$) records from Palmyra (6°N, 162°W) and Christmas (2°N, 157°W) islands to constrain central tropical Pacific ocean circulation changes during the last millennium. Seasonally to annually resolved coral $\Delta^{14}C$ measurements from the 10th, 12th–17th, and 20th centuries do not contain significant interannual to decadal-scale variations, despite large changes in coral $\delta^{18}O$ on these timescales. A centennial-scale increase in coral radiocarbon from the Medieval Climate Anomaly (~900–1200 AD) to the Little Ice Age (~1500–1800) can be largely explained by changes in the atmospheric $\Delta^{14}C$, as determined with a box model of Palmyra mixed layer $\Delta^{14}C$. However, large 12th century depletions in Palmyra coral $\Delta^{14}C$ may reflect as much as a 100% increase in upwelling rates and/or a significant decrease in the $\Delta^{14}C$ of higher-latitude source waters reaching the equatorial Pacific during this time. SEM photos reveal evidence for minor dissolution and addition of secondary aragonite in the fossil corals, but our results suggest that coral $\Delta^{14}C$ is only compromised after moderate to severe diagenesis for these relatively young fossil corals.

Citation: Zaunbrecher, L. K., K. M. Cobb, J. W. Beck, C. D. Charles, E. R. M. Druffel, R. G. Fairbanks, S. Griffin, and H. R. Sayani (2010), Coral records of central tropical Pacific radiocarbon variability during the last millennium, *Paleoceanography*, *25*, PA4212, doi:10.1029/2009PA001788.

1. Introduction

[2] Ocean circulation changes in the tropical Pacific strongly influence global climate, as demonstrated during El Niño-Southern Oscillation (ENSO) extremes. During strong El Niño events, a relaxation of the trade winds results in a large reduction of the equatorial upwelling of cooler subsurface waters and reshapes the wind-driven surface currents in the tropical Pacific [*Taft and Kessler*, 1991]. This reorganization of equatorial currents causes anomalously warm waters in the eastern and central tropical Pacific, ultimately driving a reorganization of the large-scale global atmospheric circulation. While instrumental data resolve seasonal to interannual variability in tropical Pacific circulation [*Picaut and Tournier*, 1991; *Donguy and Meyers*, 1996], the nature of decadal to centennial-scale changes in tropical Pacific circulation remain unknown. Resolving such low-frequency ocean circulation variability and its relationship to low-frequency regional and global climate changes is critical to the improvement of ocean models used for climate prediction.

[3] Radiocarbon (^{14}C) is a useful tracer of water mass mixing, as deep waters that have been isolated from the atmosphere are depleted in ^{14}C due to radioactive decay, whereas surface waters are relatively enriched. Large surface water ^{14}C gradients arise from horizontal and vertical mixing – upwelling brings relatively depleted ^{14}C waters to the ocean surface whereas prolonged air-sea gas exchange in the mid-ocean gyres drives ^{14}C enrichment in these areas. Thus, regional water masses are 'tagged' with a distinct ^{14}C signature depending on the regional oceanographic setting. Changes to regional seawater ^{14}C values through time imply changes in either horizontal or vertical mixing.

[4] Corals are useful tools for the reconstruction of seawater ^{14}C signatures as they incorporate the ^{14}C of the dissolved inorganic carbon of the seawater in which they grow into their skeletal matrix, and can live for decades to centuries [*Druffel and Linick*, 1978; *Dunbar and Cole*, 1999; *Druffel et al.*, 2007]. Annual band counting in modern corals and/or U/Th dating in fossil corals ensure accurate, ^{14}C-independent absolute chronologies for the construction of coral-based records of seawater radiocarbon variability through time. Indeed, the incorporation of "bomb ^{14}C"

[1]School of Earth and Atmospheric Sciences, Georgia Institute of Technology, Atlanta, Georgia, USA.
[2]Now at Department of Geosciences, Georgia State University, Atlanta, Georgia, USA.
[3]Physics and Geosciences Department, University of Arizona, Tucson, Arizona, USA.
[4]Scripps Institution of Oceanography, University of California, San Diego, La Jolla, California, USA.
[5]Earth System Science Department, University of California, Irvine, California, USA.
[6]Earth and Planetary Science Department, Rutgers, State University of New Jersey, New Brunswick, New Jersey, USA.

0883-8305/10/2009PA001788

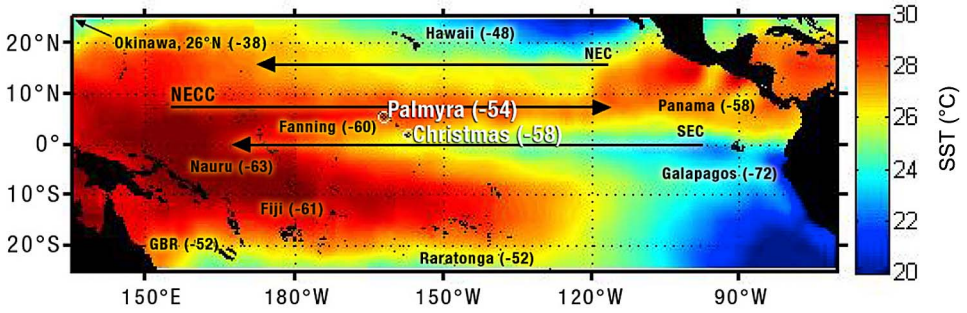

Figure 1. Map of annual average sea surface temperature in the Pacific [*Smith et al.*, 2007] (NOAA_ERSST_V3 data provided by the NOAA/OAR/ESRL PSD, Boulder, Colorado, USA, from their Web site at http://www.cdc.noaa.gov/) plotted with average prebomb Δ^{14}C as measured in corals from Galapagos [*Druffel*, 1981], Rarotonga [*Guilderson et al.*, 2000], Fiji [*Toggweiler and Dixon*, 1991], Great Barrier Reef [*Druffel and Griffin*, 1993] Panama [*Druffel*, 1987], Fanning [*Druffel*, 1987], Nauru [*Guilderson and Schrag*, *1998a*], Hawaii [*Druffel et al.*, 2001], Okinawa [*Konishi et al.*, 1981], Palmyra (this study), and Christmas (this study). Major surface ocean currents are represented by the long arrows.

[*Nydal and Loveseth*, 1983] into the surface ocean was recorded by corals across the tropics [*Grottoli and Eakin*, 2007, and references therein]. Tropical Pacific coral ^{14}C records also capture upwelling variability associated with ENSO in the postbomb interval, recording low Δ^{14}C values during La Niña events (when upwelling is strong) and high Δ^{14}C values during El Niño events (when upwelling is reduced) [*Druffel*, 1981; *Brown et al.*, 1993; *Guilderson and Schrag*, 1998b; *Guilderson et al.*, 2004]. However, with few exceptions [e.g., *Grottoli et al.*, 2003; *Druffel et al.*, 2007; *Fallon and Guilderson*, 2008], relatively little effort has been devoted to constraining prebomb ^{14}C variability in the tropical Pacific.

[5] We present Δ^{14}C records from modern and fossil corals from Palmyra (6°N, 162°W) and Christmas (2°N, 157°W) Islands to investigate changes in central tropical Pacific circulation over the last millennium. The new coral Δ^{14}C records resolve the character of interannual, decadal-, and centennial-scale seawater ^{14}C variability from the Medieval Climate Anomaly (MCA; ~900–1200 AD) through the Little Ice Age (LIA; ~1500–1800) to the 20th century. We compare the coral Δ^{14}C records to coral oxygen isotopic (δ^{18}O) climate proxy records from the same corals to probe the relationship between circulation and surface climate variability on interannual to centennial timescales. We use a box model of central tropical Pacific seawater radiocarbon to constrain the relative influence of atmospheric ^{14}C variations versus changes in ocean circulation on coral Δ^{14}C variations during the last millennium. Last, we use SEM photos to characterize the potential contribution of diagenetic processes to the fossil coral ^{14}C records.

2. Diagenetic Effects on Modern and Fossil Coral Δ^{14}C

[6] Submarine and subaerial diagenesis may alter the coral skeletal geochemistry and therefore introduce artifacts into coral paleoclimate reconstructions [*Bar-Matthews et al.*, 1993; *Enmar et al.*, 2000; *McGregor and Gagan*, 2003]. Examples of postdepositional diagenesis include dissolution, recrystallization, and/or coating by secondary aragonite or calcite. ^{14}C is especially sensitive to diagenesis involving recrystallization or secondary carbonate precipitation, because the addition of relatively young (postbomb) carbonate material to the original skeleton can add large amounts of ^{14}C [*Burr et al.*, 1992], masking the subtle prebomb ^{14}C changes associated with water mass mixing.

[7] Diagenesis of fresh coral skeleton can occur in a matter of decades, both via dissolution and/or the precipitation of secondary aragonite [*Enmar et al.*, 2000; *Hendy et al.*, 2007]. It is important to note that dissolution has no documented effect on coral Δ^{14}C or δ^{18}O, so the primary concern for the fossil corals used in this study is the recrystallization and/or precipitation of secondary aragonite and/or calcite. As the diagenetic history of the beached fossil corals used in this study is unknown, careful diagenetic screening is conducted to characterize the potential effects of diagenesis on the coral ^{14}C records.

3. Oceanographic Setting and Prebomb Δ^{14}C in the Tropical Pacific

[8] Palmyra (6°N, 162°W) and Christmas (2°N, 157°W) Islands are part of the Line Islands in the middle of the tropical Pacific Ocean (Figure 1). Palmyra lies in the path of the Northern Equatorial Counter Current (NECC), which brings warm, fresh waters eastward from the Western Pacific Warm Pool. Located nearer to the equator than Palmyra, Christmas Island is bathed in the cool, salty waters of the westward flowing Southern Equatorial Current (SEC), which carries the signature of equatorial wind-driven upwelling [*Reverdin et al.*, 1994].

[9] Coral ^{14}C records that predate the midcentury bomb testing can be used to map prebomb tropical Pacific seawater ^{14}C gradients (Figure 1). Such records reveal a roughly 20 ‰ gradient (a large signal given analytical errors of roughly ±3‰) of ^{14}C values ranging from well-equilibrated subtropical gyres at ~−50‰ to more depleted upwelling zones at ~−70‰ (Figure 1 caption and references therein). There is a roughly 20‰ zonal gradient in seawater Δ^{14}C along the

equator, with higher values in the Warm Pool and more depleted values in the eastern Pacific cold tongue. Therefore, the zonal surface currents of the tropical Pacific advect waters with significantly different ^{14}C values to the Line Island chain. The SEC brings cold, ^{14}C-depleted waters to Christmas, while the NECC contributes warmer, ^{14}C-enriched waters to Palmyra. Preliminary runs using the ^{14}C equipped GFDL MOM4 predict 8–10‰ and 10–14‰ ranges in post-bomb interannual variability in radiocarbon at Palmyra and Christmas, respectively (K. Rodgers, personal communication, 2009), although no model-based constraints exist for prebomb seawater ^{14}C variability.

4. Line Islands Coral Oxygen Isotopic Records

[10] Modern and fossil coral oxygen isotopic (δ^{18}O) records from Palmyra Island have provided detailed reconstructions of ENSO and low-frequency climate variability in the central tropical Pacific during the last millennium [*Cobb et al.*, 2001, 2003b]. The existing 20th century coral δ^{18}O records from Palmyra and Christmas islands are highly correlated to regional SST records (R = −0.65 and R = −0.84 with NIÑO3.4, respectively) [*Cobb et al.*, 2001; *Evans et al.*, 1999]. The Palmyra fossil coral δ^{18}O records reveal that during the MCA the tropical Pacific was likely cooler and/or drier than the preindustrial period, with moderate ENSO activity [*Cobb et al.*, 2003b]. The LIA was characterized by more frequent and intense ENSO events, with average climate conditions similar to preindustrial values. Generally speaking, the records reveal prominent low-frequency decadal- to centennial-scale changes in tropical Pacific climate.

[11] By comparing the existing coral δ^{18}O records to newly generated coral ^{14}C records from Palmyra and Christmas, we can investigate the relationship between surface climate (SST and hydrology) and water mass circulation on interannual to centennial timescales. One would expect that periods of stronger upwelling would be recorded as higher δ^{18}O values (signifying cooler, drier conditions) and more depleted ^{14}C (signifying the presence of deeper water at the surface). Conversely, periods of reduced upwelling might be recorded as relatively lower δ^{18}O (warmer, wetter conditions) and relatively higher Δ^{14}C (isolation of deep waters from surface). As an example, if upwelling increased at Palmyra such that SST and seawater Δ^{14}C at Palmyra were equivalent to those values at Galapagos, the change would be roughly −4°C in SST (http://www.pmel.noaa.gov/tao/data_deliv/deliv.html) and roughly −16‰ in Δ^{14}C (Figure 1). The associated changes in coral δ^{18}O and coral Δ^{14}C would be + 0.9‰ [*Epstein et al.*, 1953] and −16‰, respectively. However, it is worth noting that the signal to analytical error ratio for coral δ^{18}O in this case is roughly twice that of coral Δ^{14}C.

[12] Corals would also be sensitive to changes in the Δ^{14}C value of the upwelled waters themselves, which could be caused by changing the depth of upwelling, or by changing the source of equatorial thermocline waters. Therefore, the relationship between surface climate changes (as recorded by coral δ^{18}O) and subsurface ocean circulation change (as recorded by coral Δ^{14}C) is potentially complex. Our study provides the first well-reproduced reconstructions of interannual to centennial-scale seawater Δ^{14}C variations in the central tropical Pacific – records that can be used to refine our understanding of climate-related changes in Pacific Ocean circulation.

5. Methods

[13] For the most part, the δ^{18}O records and absolute dating constraints for the modern and fossil *Porites* corals analyzed in this study are previously published. Palmyra 'ModernB' is a duplicate core to the Palmyra modern coral record originally published by *Cobb et al.* [2001]. The Christmas modern coral (PP7–3) was originally published by *Evans et al.* [1999]. With the exception of Christmas fossil coral M2 and Palmyra fossil corals A27 and SB3B, the relevant δ^{18}O records and U/Th dates for all the fossil corals are reported by *Cobb et al.* [2003a, 2003b]. SB3B is a duplicate core of the previously published SB3 record from Palmyra [*Cobb et al.*, 2003b], while M2 and A27 will be presented by K. M. Cobb et al. (Fossil coral windows of central tropical Pacific climate over the last millennium, manuscript in preparation, 2010).

5.1. Coral δ^{18}O Measurements

[14] Most of the ^{14}C sampling was conducted on the exact slab corresponding to the published coral δ^{18}O records, whose climate-related variability guided ^{14}C sampling. However, in the case of the Palmyra modern coral and a 17th century Palmyra fossil coral (SB3), we generated new δ^{18}O profiles for duplicate slabs (referred to as 'ModernB' and 'SB3B', respectively) which were subsequently used for ^{14}C sampling. This was necessary because slab geometries and sample conservation requirements prevented us from drilling the large, closely spaced samples required for ^{14}C analysis from the original modern and SB3 slabs used by *Cobb et al.* [2001 and 2003b]. The duplicate coral δ^{18}O profiles were exactly matched to the original *Cobb et al.* [2001 and 2003b] δ^{18}O profiles (R = 0.80 for the duplicate modern cores and R = 0.64 for the duplicate SB3 cores), allowing for the assignment of firm chronological constraints. Coral powders weighing 60 to 90μg were drilled every 1mm along the coral axis of maximum growth using a table mounted, low-speed Dremel drill. The powders were analyzed for δ^{18}O on a GV Isoprime Mass Spectrometer at the Georgia Institute of Technology, with an external precision of ±0.06‰ (1σ; N = 550).

5.2. Coral Δ^{14}C Measurements

[15] The coral δ^{18}O records were used to target specific time intervals for Δ^{14}C analysis. Large amplitude ENSO, decadal, and centennial δ^{18}O variations were targeted as the likeliest periods for major circulation changes and thus the largest Δ^{14}C signals.

[16] A 1mm wide diamond-tipped bit was used in a handheld Dremel tool to drill 6–10mg of powder from coral slabs. Subannual Δ^{14}C samples were drilled every 1–3mm, corresponding to one sample every 1–2 months (~8 samples/year). Annual Δ^{14}C samples were drilled across an entire year of coral growth (10 to 25mm) guided by δ^{18}O chronologies and X-rays of the coral slabs. Coral Δ^{14}C samples were analyzed following established protocols outlined by

Druffel et al. [2004]. Coral powders were prepared for analysis by acidification to CO_2 and conversion to graphite using an Fe catalyst and the hydrogen reduction method [*Vogel et al.*, 1984]. Coral $\Delta^{14}C$ was measured on the Keck Carbon Cycle Accelerator Mass Spectrometer (KCCAMS) at the University of California, Irvine [*Southon et al.*, 2004] with a total precision of ±1.8‰ (1σ, N = 129) based on repeat measurements of an in-house coral standard (CSTD). Radiocarbon values are reported as per mil deviation from 95% of the activity of an oxalic acid standard (representing 19th century wood) as specified by *Stuiver and Polach* [1977] and age corrected to the year 1950 using published U/Th dates [*Cobb et al.*, 2003a]. The samples were corrected for fractionation using the AMS $\delta^{13}C$ and normalized to a $\delta^{13}C$ = −25‰ [*Stuiver and Polach*, 1977]. Correcting the corals' radiocarbon content using absolute U/Th ages facilitates the comparison of coral $\Delta^{14}C$ of different ages and isolates the variability of radiocarbon in the water mass at the time of coral growth.

[17] Numerous duplicates tested the reproducibility of the graphitization procedure and instrument performance. Of the first 48 samples, 9 were duplicated and all were found to agree within the errors determined by repeat measurements of a coral standard (±1.8‰, 1σ). For the rest of the study, one in ten samples was duplicated.

[18] To test the reproducibility of the University of California Irvine (UCI) coral ^{14}C measurements, 30 samples from the Palmyra and Christmas corals were measured at the University of Arizona (UA) AMS facility. Subannual samples (1mm wide solid coral slivers) were cut using a band saw from the two modern corals and three fossil corals. Sampling locations were guided by $\delta^{18}O$ chronologies and the UCI coral $\Delta^{14}C$ results to target the largest potential ^{14}C variability. Coral $\Delta^{14}C$ samples were analyzed following established protocols outlined by *Burr et al.* [1992]. Coral slivers were prepared for analysis by acidification to CO_2 and conversion to graphite using an Fe catalyst and the zinc reduction method [*Slota et al.*, 1987; *Marzaioli et al.*, 2008]. The total uncertainty for the University of Arizona coral ^{14}C measurements based on repeated measurements of an in-house coral standard is ±4.0‰ (1σ, N > 1000) [*Burr et al.*, 1998].

5.3. Diagenesis Screening by SEM and XRD

[19] A Hitachi S-800 field emission gun Scanning Electron Microscope (SEM) at the Georgia Tech Materials Science and Engineering department was used to investigate microscopic alterations to the coral skeletal morphology. Small pieces of the coral skeleton (<5mm on a side) were chipped off and mounted on SEM studs using double sided carbon tape and sputter coated with ~200Å of gold. Heavily altered coral sections identified by the SEM were ground into fine powder and examined for mineralogical content using a Philips Norelco, water-cooled XRD, type 12045, available at Georgia State University.

5.4. Mixed Layer Model of Central Tropical Pacific ^{14}C Variability

[20] In order to evaluate the potential causes of ^{14}C variability in the surface waters at Palmyra on interannual to centennial timescales, we modified a mixed layer model originally presented by *Druffel* [1997] to fit the specifics of the central tropical Pacific. The model represents an effort to quantify the various sources of ^{14}C to the central tropical Pacific surface waters through time (Figure 2). In this model, the sources of radiocarbon to the central tropical Pacific are horizontal advection, vertical advection, and air-sea CO_2 exchange.

[21] Seawater radiocarbon values in the Palmyra box evolve according to the equation:

$$P(t+\Delta t) = P(t) + [M(t) - P(t)]\Delta t + [k_{-1}A(t) - k_1 P(t)]\Delta t + W_1(t) \times \Sigma S_i \times \Delta t \times [\Sigma D_i(t) - P(t)] \quad (1)$$

where P(t) is the radiocarbon value at Palmyra at time t, M(t) is the Marine04 global ocean radiocarbon values as modeled by *Hughen et al.* [2004], Δt is the time step (1 year in this case), k_{-1} is the input rate of $^{14}CO_2$ from the air to the sea surface, k_1 is the output rate of $^{14}CO_2$ from the sea surface to the air, A(t) is the atmospheric $\Delta^{14}C$ value as reconstructed in INTCAL04 [*Reimer et al.*, 2004], $W_1(t)$ is the water mass renewal rate (set to 0.17 yr^{-1} to obtain steady state, prebomb Palmyra surface $\Delta^{14}C$ values of −54‰), S_i is the mixing constant from the deep to the surface ocean boxes (ranging from S_i = 1 at the surface to Si = 0.2 in the deepest 200m layer), and D_i is the water $\Delta^{14}C$ value in the deep boxes 1 through 7 (ranging from −54‰ at the surface to −100‰ at 200m). We integrate the model from 650 AD to 1950 AD.

[22] Horizontal advection appears to contribute ~30% of the waters entering the Palmyra box, and its radiocarbon content is assumed to follow the evolution of the globally averaged mixed layer ^{14}C estimated by *Hughen et al.* [2004]. It is important to note that alternative values for the horizontal advection component are possible, as this is poorly constrained by observations. Alternative choices (20–40%) require changes in the model upwelling rates to match prebomb ^{14}C at Palmyra. In short, no one combination of horizontal and vertical advection rates is more justifiable than another, and more importantly, changing the relative weight of horizontal versus vertical advection in the model makes little difference in the modeled ^{14}C over the last millennium. The ^{14}C value of the horizontally advected seawater tracks Marine04 [*Hughen et al.*, 2004] values for global averaged mixed layer ^{14}C, as determined by a box diffusion model which converts atmospheric ^{14}C values from dendrochronologically dated trees rings into marine mixed layer ^{14}C values. The horizontal advection component in the equatorial Pacific likely represents a combination of the Marine04 globally averaged surface waters (higher ^{14}C, better equilibrated with atmosphere) and upwelled waters (lower ^{14}C, poorly equilibrated with atmosphere) that would damp the Marine04 ^{14}C variability. Therefore, our use of Marine04 as the horizontal advection contribution represents an upper limit on the contribution of atmospheric ^{14}C variations to surface water ^{14}C variations at Palmyra through horizontal advection.

[23] Vertical advection is represented by upwelling from seven evenly spaced layers between the surface and 200m

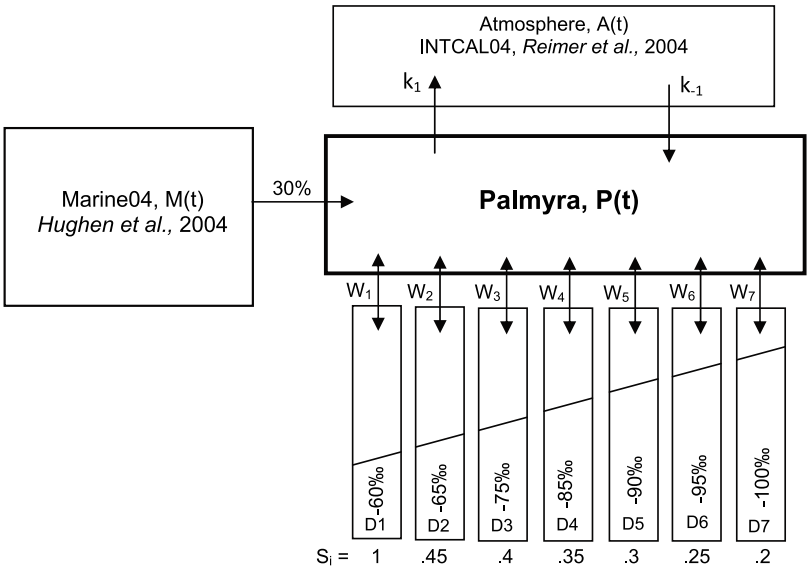

Figure 2. Schematic of the mixed layer box model used to estimate Palmyra surface Δ^{14}C over the last millennium. Horizontal advection is represented by input from box M(t) and varies through time as Marine04 [*Hughen et al.*, 2004]. Air-sea gas exchange occurs via exchange with box A(t) and varies through time as INTCAL04 [*Reimer et al.*, 2004]. Vertical advection contributes ^{14}C from deep layers D1 through D7 (20th century prebomb Δ^{14}C values are labeled), whose Δ^{14}C values are either held constant through time or are allowed to vary through time by applying Marine04-based anomalies.

deep, with Δ^{14}C values interpolated between −54‰ at the surface (the measured prebomb Δ^{14}C value at Palmyra) to −100‰ at 200m [*Rubin and Key*, 2002; *Matsumoto and Key*, 2004]. The choice of 200m as a maximum depth of upwelling is based on *Fine et al.* [1983], although some recent studies support a shallower source of upwelled waters ranging from 180m [*Bryden and Brady*, 1985] to 140m [*Weisberg and Qiao*, 2000]. In one version of the model, we hold the Δ^{14}C values of the deep water boxes fixed at the 20th century prebomb values. However, the deep water associated with equatorial upwelling is likely subducted from the extratropics several decades prior, where it experiences air-sea $^{14}CO_2$ exchange. As such, we also create a version of the model in which the deep water Δ^{14}C values evolve through time, applying the following equation:

$$D_i(t) = D_i(t) + (M_{t50} - 56‰) \quad (2)$$

where $D_i(t)$ is the deep water value at time step (t), M_{t50} is the value of Marine04 averaged from t_{-50} years to t_{-1} years, and −56‰ is the average Marine04 value from 1940 to 1950 AD. With this equation, we essentially add anomalies to each deep water layer whose magnitude is determined by the departure of Marine04 from prebomb Marine04 values, assuming a 10–50yr transit time for subducted water parcels. Fixing transit times at 50yr does not change the results by more than ±1‰, reflecting little sensitivity to choice of transit times between 50yr and 10yr.

[24] Exchange of $^{14}CO_2$ between the atmosphere and the surface ocean is governed by the exchange coefficients k_1 and k_{-1}, which depend on the atmospheric concentration of CO_2, mixed layer depth, wind speed, surface ocean total CO_2, and piston velocity [*Druffel*, 1997]. The mixed layer depth is set to 80m, which represents an intermediate value between interannual extremes of ~200m and ~0m [*Johnson et al.*, 2000]. Changing the mixed layer to 60m and 100m results in relatively small surface ocean Δ^{14}C offsets of +2‰ and −1.2‰, respectively. Wind speeds are set to 6.0 m/s, based on daily wind speed observations collected by a TAO buoy located at 5N, 155W and averaged from 1991 to 2010 (http://www.pmel.noaa.gov/tao/realtime.html), with piston velocities calculated by *Druffel* [1997]. Increasing wind speeds by ±30% resulted in prebomb ^{14}C differences of ±3‰.

[25] An inverse model is used to calculate upwelling rates (W_1) whenever coral Δ^{14}C data are available, based on inverting equation (1) and using measured Palmyra coral ^{14}C values for P(t):

$$W_1(t) = \frac{\frac{P(t+\Delta t)}{\Delta t} - \frac{P(t)}{\Delta t} - [M(t) - P(t)] - [k_{-1}A(t) - k_1 P(t)]}{[\Sigma D_i(t) - P(t)] \times \Sigma S_i} \quad (3)$$

6. Results

6.1. Interannual Coral Δ^{14}C Variability

[26] We measured Palmyra and Christmas coral Δ^{14}C across the large 1941–1943 El Niño/La Niña cycle to assess whether seawater ^{14}C is affected by ENSO-related changes in upwelling. Christmas coral Δ^{14}C data measured in 1999 by Warren Beck at UA hint at an ENSO-related signal in ocean Δ^{14}C variability, with higher Δ^{14}C during El Niño

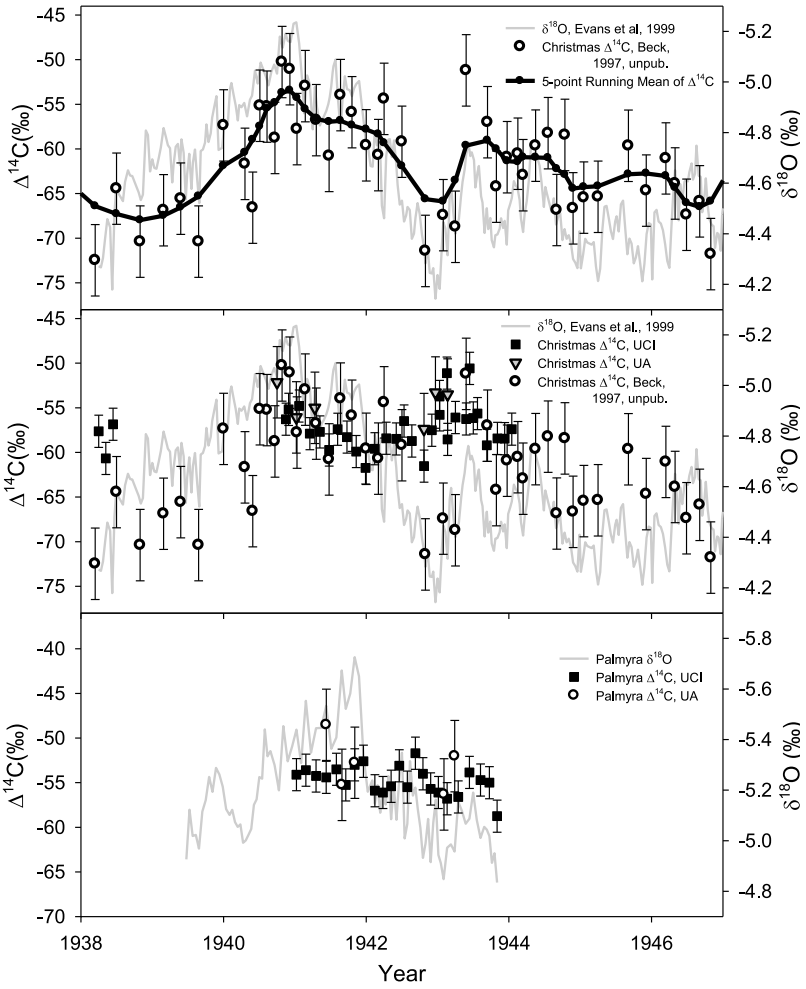

Figure 3. Christmas and Palmyra modern coral δ^{18}O and Δ^{14}C across the 1941–1943 ENSO cycle. (top) Christmas coral Δ^{14}C as measured at the University of Arizona by Warren Beck in 1997, plotted with Christmas coral δ^{18}O from *Evans et al.* [1999]. The thick black curve represents a 5 year running average of the radiocarbon data. Error is ±4.0‰ (1σ) as reported by UA. (middle) Plot of all available Δ^{14}C measurements performed on the same Christmas coral (includes UA and UCI data), plotted with coral δ^{18}O data from *Evans et al.* [1999]. Error bars for UCI coral Δ^{14}C are ±1.8‰ (1σ). (bottom) Palmyra coral Δ^{14}C as measured at UA and UCI, with respective error bars, plotted with the Palmyra 'ModernB' coral δ^{18}O (measured on duplicate core to that presented by *Cobb et al.* [2001]).

conditions (reduced upwelling) and vice versa during La Niña conditions (Figure 3, top). However, subsequent measurements on the same section of coral performed at both UA and UCI resolve no change in Christmas coral Δ^{14}C (Figure 3, middle). With the exception of one point circa 1942, the UA and UCI Christmas coral Δ^{14}C data sets agree within the 2σ analytical errors associated with each lab. At this time there is no satisfactory explanation for the slightly discrepancies between the older UA data and the newer data, which persist despite our repeated analyses of this section of coral.

[27] While the 1999 UA data suggest that there may be interannual seawater Δ^{14}C anomalies of 5–10‰ at Christmas Island, the bulk of our Christmas Island coral Δ^{14}C data suggest that these anomalies are likely smaller than 5‰. High-resolution coral Δ^{14}C measurements from Palmyra spanning the 1941–43 ENSO cycle also reveal insignificant interannual variability. A statistically significant offset (>99.9% as assessed with a student t-test) between Δ^{14}C values at Palmyra (−54.8 ± 1.6‰ stdev, n = 24) and Christmas (−58.2 ± 1.7‰ stdev, n = 24) reflects the fact that Christmas is closer to the equatorial source of ^{14}C-depleted upwelling waters, with a smaller influence of more enriched western equatorial Pacific waters. Indeed, previously published coral Δ^{14}C data from Fanning Island (4°N) fall in between the new

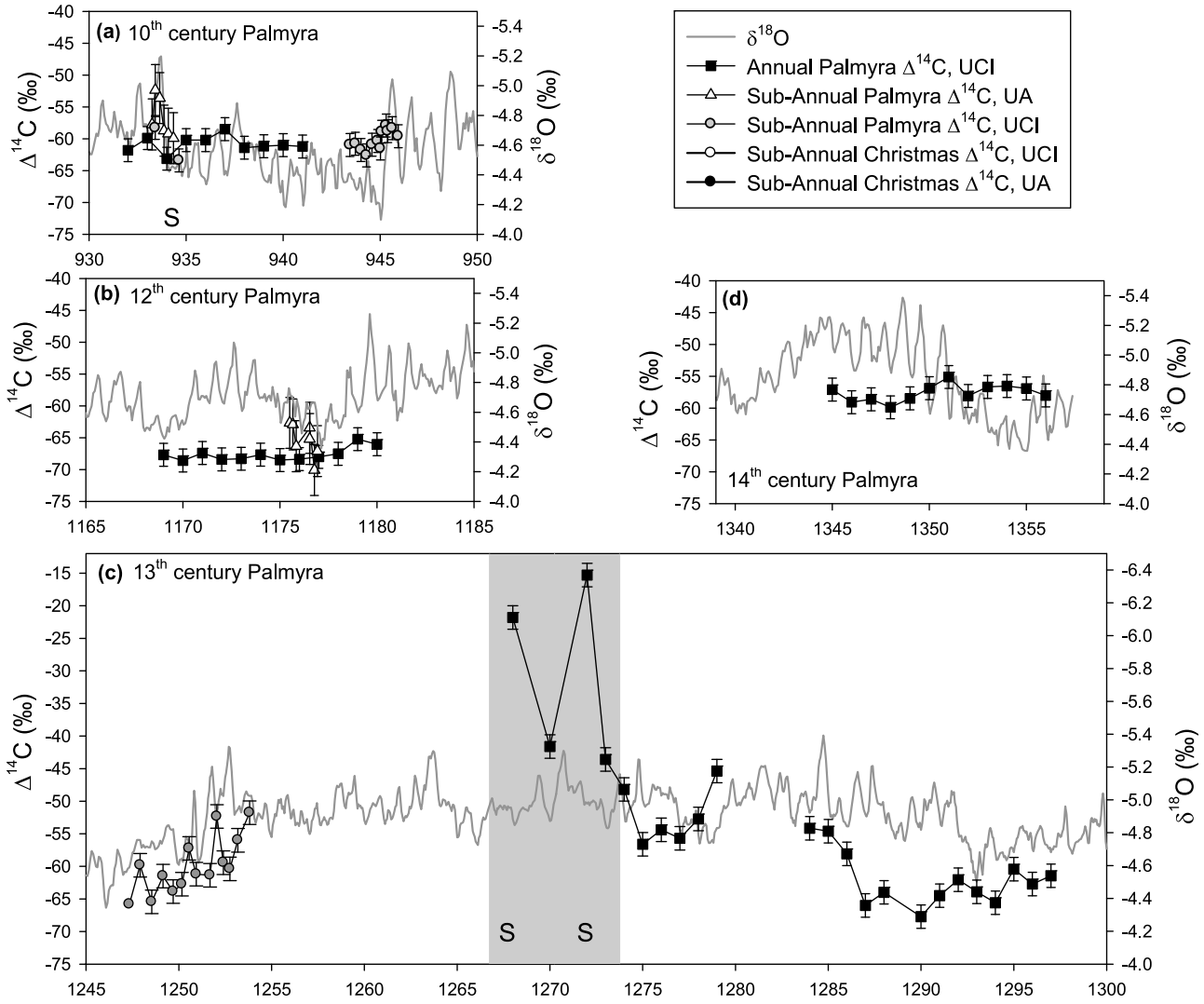

Figure 4. Comparison of Palmyra and Christmas coral ^{14}C with coral δ^{18}O. (a) The 10th century Palmyra (sample NB12), (b) 12th century Palmyra (L17), and (c) 13th century Palmyra (A27). The gray shading spans sample horizons which are associated with significant diagenetic alteration including dissolution and the addition of secondary calcite, as evidenced by SEM photos (Figure 9) and XRD analysis (not shown). Here Δ^{14}C measurements from more pristine portions of the coral represent upper limits on seawater ^{14}C during these times. A27 δ^{18}O reported by Cobb et al. (manuscript in preparation, 2010). (d) The 14th century Palmyra (SB7), (e) 15th century Palmyra (SB5), (f) 16th century Christmas (M2), (g) 17th century Palmyra (SB3B), and (h) Palmyra modern. Error bars are reported as ±1.8‰ (1σ) for UCI data and ±4.0‰ (1σ) for UA data. Palmyra coral δ^{18}O data from *Cobb et al.* [2003b]. All axes have equal scaling. 'S' marks the location of sampling horizons for SEM photos presented in Figures 7 and 8.

Palmyra and Christmas data, with an average of ~−55‰ [*Grottoli et al.*, 2003].

[28] High-resolution sampling across six additional ENSO cycles recorded in modern and fossil coral δ^{18}O data from both Palmyra and Christmas reveals similarly low interannual ^{14}C variability (Figure 4). ENSO anomalies in 1917 AD, 1655 AD, 1431–1433 AD, 1421–1422 AD, and 943–945 AD as identified by coral δ^{18}O anomalies [*Cobb et al.*, 2003b] were analyzed in Palmyra corals and an ENSO cycle in 1537–1538 AD was analyzed in a Christmas fossil coral. We conclude that interannual variations in prebomb seawater Δ^{14}C in the central tropical Pacific were smaller than the 2σ analytical error associated with these coral Δ^{14}C measurements (±3.6‰ at UCI).

6.2. Decadal Coral Δ^{14}C Variability

[29] Large decadal-scale shifts in coral δ^{18}O were targeted for Δ^{14}C analysis to investigate lower-frequency changes in surface ocean radiocarbon. Six fossil corals from Palmyra were sampled for annually averaged Δ^{14}C variations during

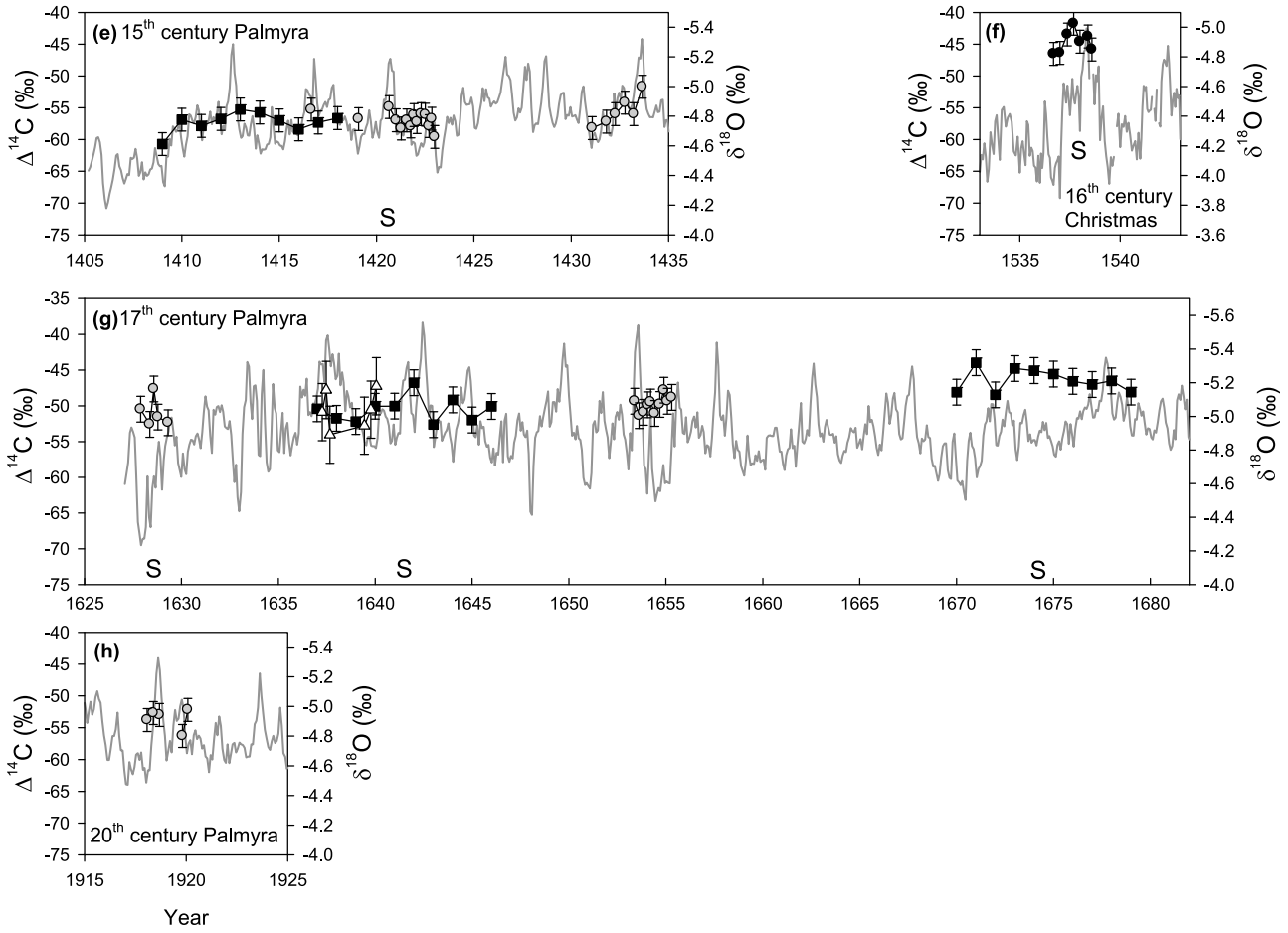

Figure 4. (continued)

932–941 AD, 1169–1180 AD, 1344–1356 AD, 1409–1418 AD, 1637–1647 AD, and 1669–1680 AD (Figure 4). The most pronounced feature in the 10th century coral $\delta^{18}O$ is a large decadal shift to heavier $\delta^{18}O$ values (cooler/drier) that occurs from 933 to 945 AD. However, coral $\Delta^{14}C$ shows no trend over this time period (Figure 4a). The 12th century annual $\Delta^{14}C$ values are similarly constant, despite a large shift in $\delta^{18}O$ from 1172 to 1180 AD (Figure 4b). Coral $\Delta^{14}C$ values from the 14th and 15th centuries range from −60.7‰ in 1409 to −55.3‰ in 1413, and do not track a significant decadal-scale change in coral $\delta^{18}O$ centered at 1350 AD (Figures 4d–4e). The mid-17th century ^{14}C values vary from −52.6‰ in 1643 to −46.8‰ in 1642, with poor correspondence to interannual to decadal-scale coral $\delta^{18}O$ variations (Figure 4g). The late 17th century $\Delta^{14}C$ values are relatively constant (Figure 4g). We conclude that seawater $\Delta^{14}C$ at Palmyra did not vary across the large decadal-scale climate anomalies inferred from coral $\delta^{18}O$ during the last millennium. See Table S1 of the auxiliary material for a full list of interannual and annual radiocarbon data.[1]

[1]Auxiliary materials are available in the HTML. doi:10.1029/2009PA001788.

6.3. Centennial Coral $\Delta^{14}C$ Variability

[30] The largest signal in the Line Island coral $\Delta^{14}C$ reconstructions is a centennial-scale rise in $\Delta^{14}C$ that occurs from the MCA to the LIA. In comparison to modern pre-bomb $\Delta^{14}C$ values of −54.8‰ ± 1.6 (n = 3, where n is the number of years included in the average, see Table 1) at Palmyra, 12th and 13th centuries are associated with the most depleted radiocarbon values of those sampled during the millennium, averaging −67.6‰ ± 1.0 (n = 12) and −61.5‰ ± 4.0 (n = 20), respectively (Figure 5 and Table 1). It is important to note that the 13th century coral contains appreciable secondary aragonite (see section 6.5), which means that the measured ^{14}C values represent an upper limit on seawater radiocarbon during this time. Values during the LIA are higher with respect to the MCA and early 20th century, ranging from −50.5‰ ± 1.5 (n = 16) in the mid-17th century at Palmyra to −45.0 ± 1.4 (n = 3) in the mid 16th century at Christmas (Figure 5 and Table 1). $\Delta^{14}C$ values of Palmyra coral in the 10th, 14th, and 15th centuries [−60.8 ± 1.2‰ (n = 13), −57.6 ± 1.3‰ (n = 12) and −56.9 ± 1.5‰ (n = 16), respectively] are similar to early 20th century $\Delta^{14}C$ values.

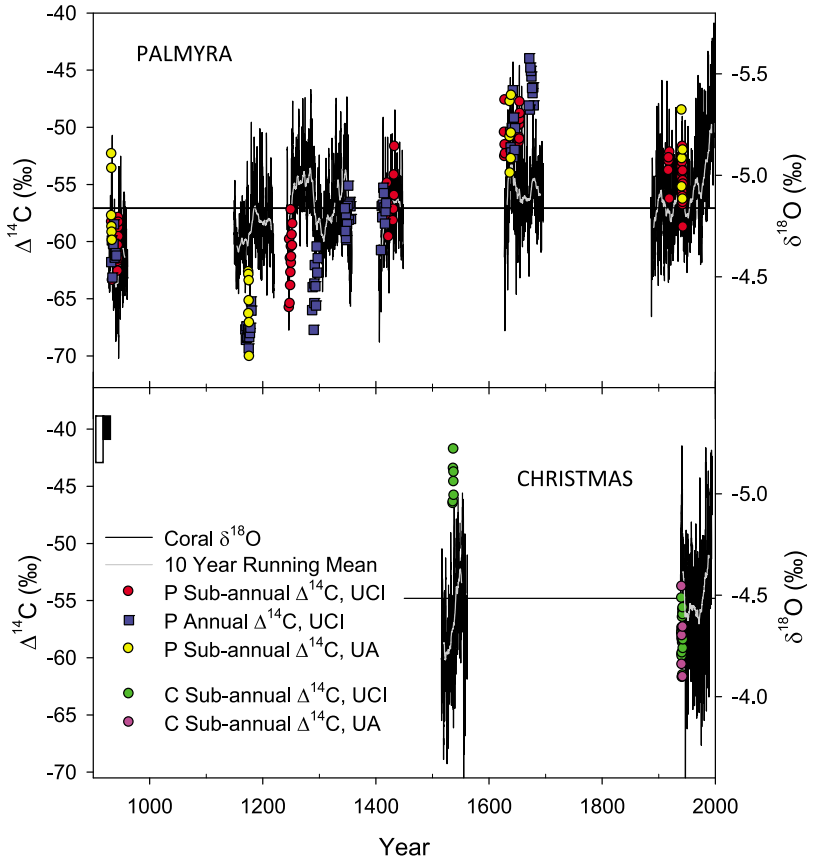

Figure 5. Summary of Palmyra (P) and Christmas (C) modern and fossil coral δ^{18}O and Δ^{14}C over the last millennium. The black vertical bar represents the ±1.8‰ UCI AMS error; the vertical white bar represents the ±4.0‰ UA AMS error. The horizontal black lines indicate both the average δ^{18}O and Δ^{14}C values of the respective island's data. The gray line represents a 10 year running average of the coral δ^{18}O data.

6.4. Mixed Layer Model Constraints on the Sources of Coral Δ^{14}C Variability Over the Last Millennium

[31] The Palmyra mixed layer model suggests that atmospheric Δ^{14}C variations explain most, though not all, of the centennial-scale Δ^{14}C variability recorded in the Palmyra and Christmas fossil corals (Figure 6).

[32] Twelfth and late 13th century coral Δ^{14}C values that are significantly lower than the mixed layer model prediction may indicate increased sensitivity to low atmospheric Δ^{14}C values during this time and/or changes in ocean circulation. It is important to note that the absolute ages of the 12th century coral would have to shift by 50–70 years in order for the Δ^{14}C data to match the mixed layer model prediction, far beyond the ±10yr chronological errors associated with this coral [*Cobb et al.*, 2003b]. However, the Marine04 curve used in the mixed layer model significantly damps relatively low atmospheric Δ^{14}C values during the 12th century, likely because the Δ^{14}C gradient between the atmosphere and mixed layer is relatively small during this time period. In general, the smoothed atmospheric Δ^{14}C curve overpredicts the observed coral Δ^{14}C variability over the last millennium (most notably during the 10th and 16th centuries), but is a better match for the 12th century coral data than the Marine04-derived prediction. Therefore, the 12th century coral data may reflect a heightened sensitivity to atmospheric Δ^{14}C variability during this time (which in turn may be linked to changes in ocean circulation). If the mixed layer model accurately represents the incorporation of atmospheric Δ^{14}C anomalies into the surface ocean, however, we infer that changes in ocean circulation occurred during the 12th and late 13th centuries.

6.5. Diagenesis in the Line Island Fossil Corals

[33] The majority of the Palmyra coral collection was previously examined for diagenesis using XRD and thin sections [*Cobb*, 2002], but these techniques cannot resolve subtle diagenesis that could introduce artifacts into coral-based seawater ^{14}C reconstructions. A pristine coral skeleton has a smooth, solid surface with easily identifiable dissepiments, and unfilled pore spaces (Figure 7a). Secondary aragonite deposition in corals occurs as tiny needles protruding from the original skeleton into open pore spaces, and is commonly associated with submarine diagenesis [*Enmar et al.*, 2000; *Hendy et al.*, 2007]. SEM photos suggest that the modern Palmyra coral, 10th century coral (NB12), 12th century coral (L17),14th century coral (SB7), 15th century coral (SB5), and 16th century Christmas coral (M2) all retain relatively

Table 1. Absolute Ages, Average Annual Δ^{14}C Values, and Average δ^{18}O Values for the Palmyra and Christmas Modern and Fossil Corals

Sample	Island[a]	Absolute Age Assignment[b]	AMS	Δ^{14}C[c] (‰)	δ^{18}O[d] (‰)
NB12	P	928–961 (±10 yr)	UCI	−60.8 ± 1.19 (n = 13, N = 24)	−4.58
			UA	−57.6 ± 2.79 (n = 2, N = 5)	
L17	P	1149–1220 (±10 yr)	UCI	−67.6 ± 1.03(n = 12, N = 12)	−4.73
			UA	−65.6 ± 2.26(n = 2, N = 6)	
A27[e]	P	1242–1330 (±5 yr)	UCI	−61.5 ± 4.02(n = 20, N = 35)	−4.86
SB7	P	1326–1357 (±5 yr)	UCI	−57.6 ± 1.32(n = 12, N = 12)	−4.83
SB5	P	1405–1448 (±5 yr)	UCI	−56.9 ± 1.54 (n = 16, N = 30)	−4.78
M2[e]	C	1515–1561(±5 yr)	UCI	−45.0 ± 1.36 (n = 3, N = 7)	−4.36
SB3B	P	1627–1658 (±5 yr)	UCI	−50.5 ± 1.50 (n = 16, N = 25)	−4.85
			UA	−49.9 ± 2.36 (n = 3, N = 6)	
SB13	P	1653–1695 (±5 yr)	UCI	−46.4 ± 1.54 (n = 10, N = 10)	−4.90
Modern	P	1918–1920 (±2 months)	UCI	−53.9 ± 2.14 (n = 3, N = 5)	−4.91
ModernB	P	1938–1944 (±2 months)	UCI	−54.8 ± 1.07 (n = 3, N = 24)	−4.91
			UA	−53.2 ± 1.41 (n = 2, N = 5)	
PP7–3	C	1938–1993 (±2 months)	UCI	−58.0 ± 0.71 (n = 4, N = 24)	−4.51
			UA	−54.1 ± 1.61 (n = 4, N = 6)	

[a]P, Palmyra Island; C, Christmas Island.
[b]U/Th dates and uncertainties reported by *Cobb et al.* [2003a]. Palmyra modern coral age model reported by *Cobb et al.* [2001]. Christmas modern coral age model reported by *Evans et al.* [1999].
[c]Errors represent the 1σ standard deviation of all available coral Δ^{14}C measurements for a given coral. Analytical error of UCI radiocarbon measurements is ±1.8‰ (1σ). Analytical error for UA radiocarbon measurement is ±4.0‰ (1σ). In parentheses, n is the number of years represented in the average, N is the total number of samples, subannual samples were averaged into annual values and included where possible.
[d]Average coral δ^{18}O. Analytical error for coral δ^{18}O is ±0.06‰ (1σ).
[e]Unpublished U/Th ages and δ^{18}O data for fossil corals A27 and M2 to be reported by Cobb et al. (manuscript in preparation, 2010).

pristine coral skeletons lacking obvious signs of secondary aragonite deposition and/or major dissolution (Figures 7b–7e).

[34] As secondary aragonite precipitation would cause an enrichment in coral Δ^{14}C values, we used SEM photos to determine whether diagenesis could have caused the relatively large ^{14}C enrichments observed in the 16th and 17th century fossil corals. Indeed, SEM photos of 17th century Palmyra coral SB3B reveal areas in the oldest portion of the core that are covered in small secondary aragonite needles (Figure 8a). Radiocarbon values from this horizon average −50.9‰ (±2.0, N = 6). However, samples taken from younger sections in the same coral lack any evidence of diagenesis, yet are similarly enriched in ^{14}C (averaging −49.8‰, ± 1.1, N = 12) (Figure 8b). Furthermore, the late 17th century coral (SB13) is even higher in Δ^{14}C than SB3B, yet shows no signs of diagenesis (Figure 7d). SEM photos also rule out the influence of diagenesis on the very high Δ^{14}C values measured in the 16th century Christmas fossil coral M2 (−45.0‰, ± 1.4, n = 3). Taken together, these lines of evidence suggest that the minor diagenesis observed in one LIA fossil coral did not significantly affect the Δ^{14}C values of this coral.

[35] Moderate to severe diagenesis in a 13th century fossil coral (A27) was associated with Δ^{14}C values as high as −21‰, far outside the expected range of seawater Δ^{14}C values in the surface ocean. Such high coral Δ^{14}C values can only be explained by the addition of relatively young secondary carbonates to the original coral skeleton. In fact, mass balance calculations suggest that portions of this coral must be contaminated with as much as 50% of early 20th century carbonates to obtain values approaching −21‰. Of course, if the contaminating material contains bomb radiocarbon, less material would be required to cause the observed enrichments. SEM photos of A27 revealed severe

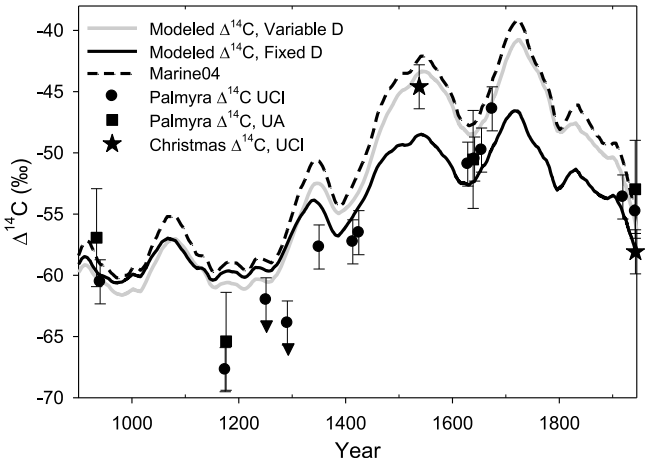

Figure 6. Comparison of Palmyra mixed layer model Δ^{14}C with measured Palmyra and Christmas coral Δ^{14}C over the last millennium. Palmyra mixed layer model output for fixed (solid black line) and variable (solid gray line) Δ^{14}C values for deep water boxes are plotted with Marine04 [*Hughen et al.*, 2004] (dashed line) and average measured coral Δ^{14}C values for each modern and fossil coral segment. Error bars represent the analytical errors of ±1.8‰ for data generated at UCI, or ±4.0‰ for data generated at UA. The 13th century fossil coral Δ^{14}C are plotted as maximum values, as secondary carbonates with higher Δ^{14}C contaminate this coral (downward arrows reflect the fact that the primary coral Δ^{14}C are likely lower than the Δ^{14}C values measured).

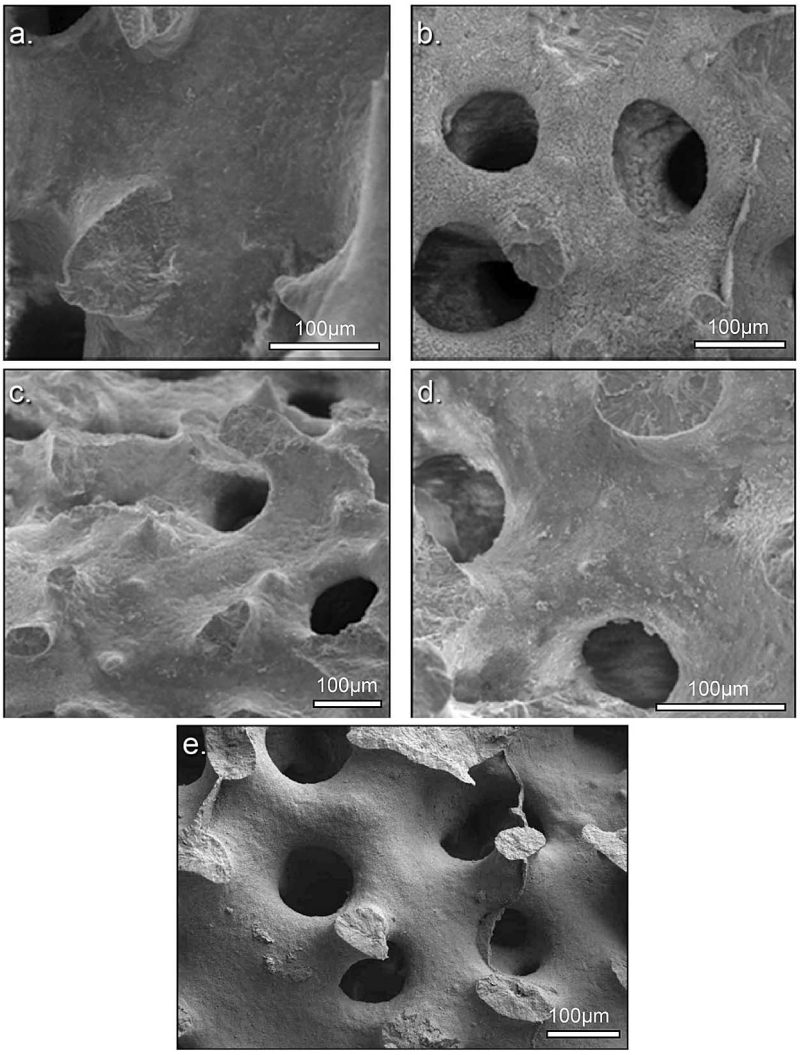

Figure 7. SEM photos of pristine modern and fossil corals. (a) Palmyra ModernB (sampled at a depth corresponding to ~1942 AD), (b) Palmyra fossil coral NB12 (~930 AD) showing signs of minor dissolution, (c) Palmyra fossil coral SB5 (~1430 AD), (d) Palmyra fossil coral SB13 (~1760 AD), and (e) Christmas fossil coral M2 (~1550 AD). L17 and SB7 photos not shown.

dissolution in parts of the coral (Figure 9a) in conjunction with smooth, platy crystals that cover large sections of the coral skeleton (Figures 9b–9d). XRD analysis of the most altered portion of A27 revealed the presence of calcite, as sometimes observed in much older, heavily altered fossil corals [e.g., *McGregor and Gagan*, 2003]. The Δ^{14}C values obtained for more pristine portions of this coral (Figure 8) are interpreted as upper limits on seawater Δ^{14}C during this time, as diagenesis may be masking lower Δ^{14}C during this time.

7. Discussion

7.1. Interannual Δ^{14}C Variability in the Central Tropical Pacific

[36] Palmyra and Christmas coral Δ^{14}C values are unchanged throughout multiple large ENSO cycles over the last millennium, including the very large 1941–43 ENSO cycle. The lack of interannual Δ^{14}C variability indicates that the surface ocean in the central tropical Pacific is relatively well mixed with respect to ^{14}C, at least to the depth of wind-driven upwelling, and to the limit of current analytical precisions for Δ^{14}C. Indeed, *Toggweiler and Carson* [1995] use a model of nitrate and carbon concentrations in the surface ocean to demonstrate that the NECC and SEC are not distinguishable in the central tropical Pacific on interannual timescales due to the effective mixing of surface waters in this region, both horizontally and vertically. Indeed, for many geochemical tracers, such as ^{14}C, the zonal structures of the NECC and the SEC are clear only in multiyear averages. *Toggweiler and Carson* [1995] find that at this particular site in the central tropical Pacific, seawater Δ^{14}C is homogenous to depths of 150m, roughly equivalent to the depth of upwelling. If this is correct, then changes in interannual upwelling and/or horizontal advection in the

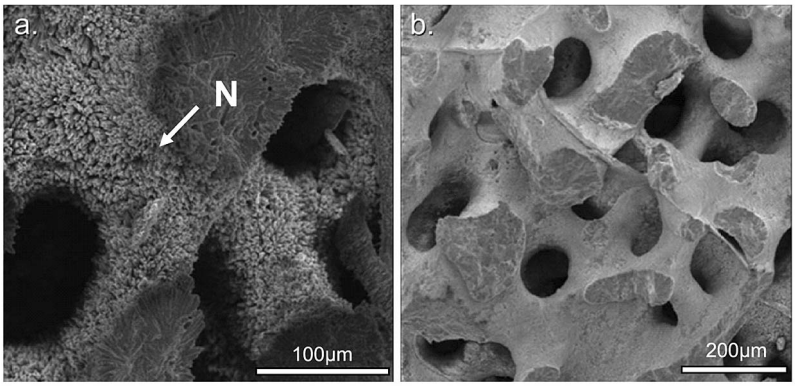

Figure 8. SEM photos of Palmyra fossil coral SB3B taken (a) from the base of the core, where many secondary aragonite needles cover the original surface of the coral skeleton and (b) midway up the core, where the skeleton is smooth and retains the original skeletal structure. N denotes secondary aragonite needles.

vicinity of Palmyra and Christmas Islands would not be expected to significantly change seawater Δ^{14}C at these sites. It is important to note that heat is exchanged much more rapidly across the air-sea interface than carbon dioxide (1–2 months versus ~10 years for ^{14}C equilibration), meaning that water masses of different heat contents can possess similar Δ^{14}C signatures. Therefore, ENSO-related upwelling events are associated with changes in SST but not necessarily with changes in seawater Δ^{14}C.

[37] The lack of an interannual Δ^{14}C signal at Palmyra is supported by a coral Δ^{14}C reconstruction from nearby Fanning Island (4°N, 154°W), which shows little to no interannual Δ^{14}C variations [*Grottoli et al.*, 2003]. We are left to conclude that if central equatorial seawater Δ^{14}C may vary across an ENSO cycle, the associated signal (<5 ‰) is not large enough to be captured using current analytical techniques (i.e., a low signal-to-noise ratio). This can be contrasted with coral δ^{18}O, which can resolve ENSO-related

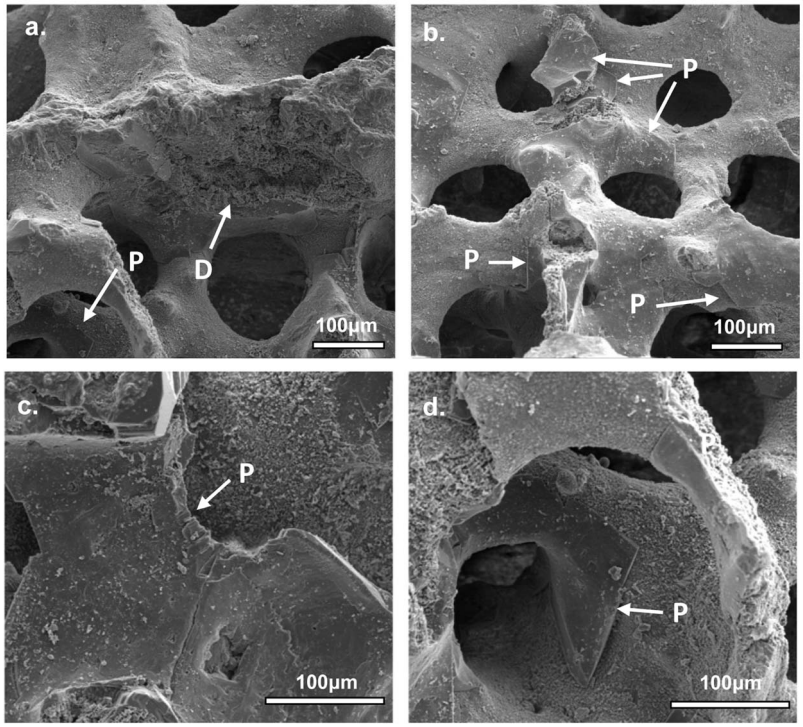

Figure 9. SEM photos of diagenesis in 13th century Palmyra fossil coral A27. (a) Section of coral skeleton characterized by massive dissolution (marked by 'D'); (b) solid, platy crystals (marked by 'P') covering large sections of the original coral skeleton, identified as calcite by XRD (not shown). (c and d) Enlarged views of platy diagenetic crystals in A27.

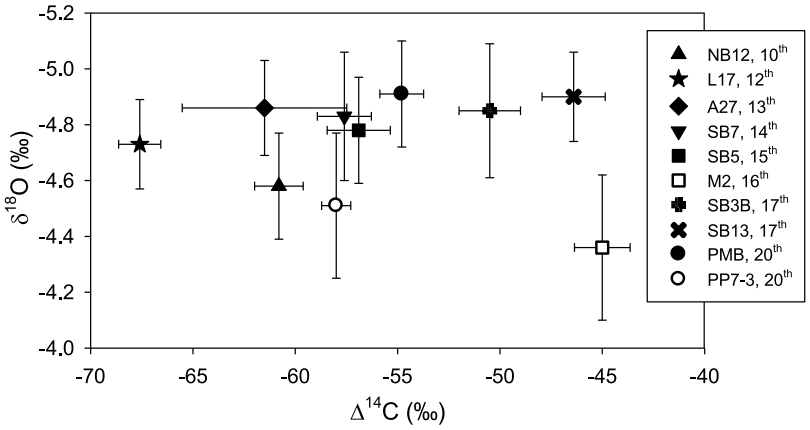

Figure 10. Plot of average coral $\Delta^{14}C$ and $\delta^{18}O$ for each coral, computed over the intervals where $\Delta^{14}C$ data were collected. $\Delta^{14}C$ error bars reflect the 1σ spread of the annually averaged coral ^{14}C for each sequence (as presented in Table 1) and $\delta^{18}O$ error bars reflect the 1σ spread of the annually averaged coral $\delta^{18}O$ data computed over the same time intervals as the $\Delta^{14}C$ data.

SST changes of ±1–3°C (±0.2–0.6 ‰) that occur in this region, given analytical errors of ±0.06‰.

7.2. Decadal to Centennial $\Delta^{14}C$ Variability in the Central Tropical Pacific

[38] Large decadal signals in coral $\delta^{18}O$ data are not associated with significant coral $\Delta^{14}C$ variability, indicating a decoupling between surface climate and seawater $\Delta^{14}C$ on decadal timescales. This is somewhat surprising, and cannot be explained by different equilibration times of ocean heat versus ^{14}C, as invoked above to explain the lack of interannual ^{14}C variability. One possibility is that surface climate signals and basin-scale circulation reorganizations are lagged by as much as a decade. In other words, a climate signal that originates at the equator might influence higher-latitude climate fairly quickly, but it might take many years for the changes in high-latitude climate and circulation to make their way into the equatorial thermocline. Such a mechanism has previously been proposed to explain Pacific decadal-scale climate variability [e.g., *Gu and Philander*, 1997], and may underlie the lack of simultaneous changes in coral $\delta^{18}O$ and coral $\Delta^{14}C$ observed here.

[39] Support for a climate $\Delta^{14}C$ delay comes from modeling studies that suggest that variability associated with the relatively ^{14}C-depleted Subantarctic Mode Waters (SAMW) may have a large, but delayed impact on the ^{14}C content of equatorial thermocline waters in the tropical Pacific [*Rodgers*, 2003]. Indeed, the *Rodgers* [2003] study indicates that up to 70% of the water reaching the equatorial mixed layer originates in the Southern Hemisphere, where surface radiocarbon values can be as low as −100‰ [*Matsumoto and Key*, 2004]. However, it likely takes as long as 30 years for waters subducted as part of the SAMW to reach the equator [*Rodgers*, 2003], potentially explaining why surface climate changes (as recorded in coral $\delta^{18}O$) and seawater ^{14}C changes (as recorded by coral ^{14}C) in the tropical Pacific could be offset by several decades.

[40] A comparison of the centennial-scale coral $\delta^{18}O$ and $\Delta^{14}C$ records reveals a poor correlation between reconstructed surface climate and inferred paleocirculation (Figure 10). For example, relatively depleted coral $\Delta^{14}C$ anomalies during the 12th century are not associated with positive coral $\delta^{18}O$ anomalies, as expected if upwelling variations were responsible for the coral $\Delta^{14}C$ shift. The decoupling of $\delta^{18}O$ and $\Delta^{14}C$ cannot be explained by alterations to the coral skeleton, as the 12th century coral is free of diagenesis. Given the absence of coral $\delta^{18}O$ anomalies on these timescales, we infer that changes in high-latitude source water $\Delta^{14}C$ signatures caused the observed coral ^{14}C anomalies rather than changes in equatorial Pacific upwelling. Relatively small changes in either the $\Delta^{14}C$ of SAMW waters or their relative contribution to the equatorial undercurrent could have caused the ~7‰ departures from the atmospheric ^{14}C-driven mixed layer model curve. In this case, we infer a $\Delta^{14}C$ decrease in SAMW (or an increase of SAMW contributions to the EUC) during the 12th century. Likewise, relatively enriched coral radiocarbon during the 16th and 17th centuries could result from a reduction in the amount of SAMW reaching the equatorial mixed layer and/or an increase in the $\Delta^{14}C$ of SAMW.

[41] Using the inverse version of the Palmyra mixed layer model, we calculate that a twofold increase in upwelling rates would explain the anomalously depleted 12th century Palmyra coral $\Delta^{14}C$ values (not shown). Our simple box model does not constrain the influence of potential changes in high-latitude source water ^{14}C content or circulation that could also account for the observed centennial-scale coral ^{14}C variability. Ultimately, the relationship between low-frequency equatorial climate and high-latitude circulation must be tested with ^{14}C-equipped coupled ocean-atmosphere climate models run for multiple centuries.

7.3. Diagenetic Effects on Coral $\Delta^{14}C$

[42] As discussed previously, the addition of calcite or secondary aragonite to the original coral skeleton introduces younger, relatively ^{14}C-enriched carbonate to the coral skeleton. The magnitude of the diagenetic ^{14}C enrichment depends on the amount of secondary carbonate precipitated, and its age relative to the primary coral skeleton. Diagenetic

alterations to 17th century Palmyra coral SB3B include secondary aragonite needles in the lower section of the core, although these needles do not significantly alter coral $\Delta^{14}C$ values relative to pristine portions of the core. However, it is difficult to generate large $\Delta^{14}C$ anomalies over a ~400 year period – it would require a 10% addition of modern prebomb carbonate to raise 17th century coral $\Delta^{14}C$ values by 4‰. A 10% addition of 18th century carbonate to the 17th century coral would result in an undetectable change in coral $\Delta^{14}C$. In agreement with our results, *Cohen and Hart* [2004] find that secondary aragonite precipitation did not affect the fidelity of their fossil coral radiocarbon ages (~13,500 years old) concluding that the diagenesis must have occurred shortly after skeletal formation. Although many coral paleoclimate proxies can be altered by secondary aragonite precipitation or dissolution [i.e., *Hendy et al.*, 2007], we conclude that the radiocarbon signatures of young (<1000 years old), relatively pristine fossil coral are not significantly affected.

[43] In the case of the 13th century fossil coral that experienced significant diagenesis (both dissolution and secondary calcite precipitation), coral $\Delta^{14}C$ values were significantly higher. Previous work indicates that secondary calcite should also cause significant enrichments in coral $\delta^{18}O$ [*Enmar et al.*, 2000; *Müller et al.*, 2001; *McGregor and Gagan*, 2003], which were not observed in this study. This implies a markedly different mechanism of diagenetic alteration than observed in the other fossil corals – one that progressed continuously as the coral lay exposed on the beach over the last seven centuries.

[44] We conclude that the accuracy of modern or fossil coral-based seawater $\Delta^{14}C$ reconstructions depends on careful diagenetic screening, ideally with SEM photos. As a screening tool, SEM is far preferable to thin sections, as the small needles of secondary aragonite observed in SEM photos of SB3B were not observed in thin section.

8. Conclusions

[45] Despite large variations in interannual to decadal surface climate inferred from modern and fossil coral $\delta^{18}O$, we find no corresponding changes in coral $\Delta^{14}C$, suggesting that these two tracers have markedly different sensitivities and/or response times in the central tropical Pacific. In the case of interannual variability, the relatively long air-sea equilibration time of ^{14}C versus heat means that the horizontal and vertical $\Delta^{14}C$ gradients are generally smaller than they are for SST, which is exacerbated by relatively large error bars for seawater $\Delta^{14}C$ reconstructions. In the case of decadal-scale variations, the potential for changes in the ^{14}C content of extratropical waters that supply the tropical Pacific thermocline waters represents an added complication, as such changes may lead or lag changes in tropical Pacific surface climate by several decades. A centennial-scale increase in coral $\Delta^{14}C$ from the MCA to the LIA is largely explained by centennial-scale changes in atmospheric $\Delta^{14}C$. However, 12th and late 13th century coral $\Delta^{14}C$ data are more depleted than atmospheric $\Delta^{14}C$-driven mixed layer model estimates. If the mixed layer model accurately represents the incorporation of very low 12th century atmospheric $\Delta^{14}C$ values into the Palmyra mixed layer, then the 12th century coral data imply an increase in upwelling during this time and/or a decrease in the ^{14}C content of equatorial source waters, requiring further study with ^{14}C-equipped ocean models. Minor dissolution and addition of secondary aragonite, as observed with SEM photos, has little effect on the accuracy of our coral-based seawater ^{14}C reconstructions. However, moderate to severe diagenesis (marked by extensive dissolution and the addition of secondary calcite) is associated with significantly higher $\Delta^{14}C$ values.

[46] **Acknowledgments.** We thank Rick Mortlock for providing the modern Christmas coral PP7–3 used in this study and Mike Evans for providing the corresponding raw $\delta^{18}O$ data. John Southon and Guaciara dos Santos of the KCCAMS Facility facilitated our UC Irvine AMS measurements. We are grateful to Crawford Elliott for providing quick access to XRD. Discussions with Keith Rodgers, Robbie Toggweiler, and Jean Lynch-Stieglitz greatly improved the quality of this manuscript. Thanks to TAO Project Office of NOAA/PMEL for wind speed data. Funding for this project was provided to KMC by NSF award OCE-0452920 and to ERMD by NSF awards OCE-0502619 (Earth System History) and OCE-0551940 (Chemical Oceanography).

References

Bar-Matthews, M., G. J. Wasserburg, and J. H. Chen (1993), Diagenesis of fossil coral skeletons: Correlation between trace elements, textures, and ^{234}U / ^{238}U, *Geochim. Cosmochim. Acta*, *57*, 257–276, doi:10.1016/0016-7037(93)90429-Z.

Brown, T., G. W. Farwell, P. M. Grootes, F. H. Schmidt, and M. Stuvier (1993), Intra-annual variability of the radiocarbon of corals from the Galapagos Islands, *Radiocarbon*, *35*, 245–251.

Bryden, H. L., and E. C. Brady (1985), Diagnostic model of three-dimensional circulation in the upper equatorial Pacific Ocean, *J. Phys. Oceanogr.*, *15*, 1255–1273, doi:10.1175/1520-0485(1985)015<1255:DMOTTD>2.0.CO;2.

Burr, G. S., R. L. Edwards, D. J. Donahue, E. R. M. Druffel, and F. W. Taylor (1992), Mass spectrometric ^{14}C and U-Th measurements in coral, *Radiocarbon*, *34*, 611–618.

Burr, G. S., J. W. Beck, F. W. Taylor, J. Recy, R. L. Edwards, G. Cabioch, T. Correge, D. J. Donahue, and J. M. O'Malley (1998), A high resolution radiocarbon calibration between 11,700 and 12,400 calendar years BP derived from ^{230}Th ages of corals from Espiritu Santo Island, Vanuatu, *Radiocarbon*, *40*, 1093–1105.

Cobb, K. M. (2002), *Coral records of the El Niño-Southern Oscillation and tropical Pacific climate over the last millennium*, Ph.D. dissertation, Univ. of Calif., San Diego.

Cobb, K. M., D. E. Hunter, and C. D. Charles (2001), A central tropical Pacific coral demonstrates Pacific, Indian, and Atlantic decadal climate connections, *Geophys. Res. Lett.*, *28*(11), 2209–2212, doi:10.1029/2001GL012919.

Cobb, K. M., C. D. Charles, H. Cheng, M. Kastner, and R. L. Edwards (2003a), U/Th-dating living and young fossil corals from the central tropical Pacific, *Earth Planet. Sci. Lett.*, *210*, 91–103, doi:10.1016/S0012-821X(03)00138-9.

Cobb, K. M., C. D. Charles, H. Cheng, and R. L. Edwards (2003b), El Niño-Southern Oscillation and tropical Pacific climate during the last millennium, *Nature*, *424*, 271–276, doi:10.1038/nature01779.

Cohen, A. L., and S. R. Hart (2004), Deglacial sea surface temperatures of the western tropical Pacific: A new look at old coral, *Paleoceanography*, *19*, PA4031, doi:10.1029/2004PA001084.

Donguy, J. R., and G. Meyers (1996), Mean annual variation of transport of major currents in the tropical Pacific Ocean, *Deep Sea Res., Part I*, *43*(7), 1105–1122, doi:10.1016/0967-0637(96)00047-7.

Druffel, E. R. M. (1981), Radiocarbon in annual coral rings from the eastern tropical Pacific Ocean, *Geophys. Res. Lett.*, *8*, 59–62, doi:10.1029/GL008i001p00059.

Druffel, E. R. M. (1987), Bomb radiocarbon in the Pacific: Annual and seasonal timescale variations, *J. Mar. Chem.*, *45*, 667–698.

Druffel, E. R. M. (1997), Pulses of rapid ventilation in the North Atlantic surface ocean during the past century, *Science*, *275*, 1454–1457.

Druffel, E. R. M., and S. Griffin (1993), Large variations of surface ocean radiocarbon: Evidence of circulation changes in the southwestern Pacific, *J. Geophys. Res.*, *98*(C11), 20,249–20,259, doi:10.1029/93JC02113.

Druffel, E. R. M., and T. W. Linick (1978), Radiocarbon in annual coral rings of Florida, *Geophys. Res. Lett.*, *5*(11), 913–917, doi:10.1029/GL005i011p00913.

Druffel, E. R. M., S. Griffin, T. P Guilderson, M. Kashgarian, J. Southon, and D. P. Schrag (2001) Changes of subtropical north Pacific radiocarbon and correlation with climate variability, *Radiocarbon*, *43*(1), 15–25.

Druffel, E. R. M, S. Griffin, J. Hwang, T. Komada, S. R. Beaupre, K. C. Druffel-Rodriguez, G. M. Santos, and J. Southon (2004), Variability of radiocarbon during the 1760s in monthly corals from the Galapagos Islands, *Radiocarbon*, *46*, 627–632.

Druffel, E. R. M., S. Griffin, S. R. Beaupre, and R. B. Dunbar (2007), Oceanic climate and circulation changes during the past four centuries from radiocarbon in corals, *Geophys. Res. Lett.*, *34*, L09601, doi:10.1029/2006GL028681.

Dunbar, R. G., and J. E. Cole (1999), Annual records of tropical systems (ARTS), *Workshop Rep.*, 99-1, 72 pp., Past Global Changes, Bern.

Enmar, R., M. Stein, M. Bar-Matthews, E. Sass, A. Katz, and B. Lazar (2000), Diagenesis in live corals from the Gulf of Aqaba. I. The effect on paleo-oceanography tracers, *Geochim. Cosmochim. Acta*, *64*(18), 3123–3132, doi:10.1016/S0016-7037(00)00417-8.

Epstein, S., R. Buchsbaum, H. A. Lowenstam, and H. C. Urey (1953), Revised carbonate-water isotopic temperature scale, *Geol. Soc. Am. Bull.*, *64*, 1315–1326, doi:10.1130/0016-7606.

Evans, M. N., R. G. Fairbanks, and J. L. Rubenstone (1999), The thermal oceanographic signal of ENSO reconstructed from a Kiritimati Island coral, *J. Geophys. Res.*, *104*, 13,409–13,421, doi:10.1029/1999JC900001.

Fallon, S. J., and T. P. Guilderson (2008), Surface water processes in the Indonesian throughflow as documented by a high resolution coral Δ^{14}C record, *J. Geophys. Res.*, *113*, C09001, doi:10.1029/2008JC004722.

Fine, R. A., W. H. Peterson, C. G. H. Rooth, and H. G. Ostlund (1983), Cross-equatorial tracer transport in the the upper waters of the Pacific Ocean, *J. Geophys. Res.*, *88*, 763–769, doi:10.1029/JC088iC01p00763.

Grottoli, A. G., and C. M. Eakin (2007), A review of modern coral δ^{18}O and Δ^{14}C proxy records, *Earth Sci. Rev.*, *81*, 67–91, doi:10.1016/j.earscirev.2006.10.001.

Grottoli, A. G., S. T. Gille, E. R. M. Druffel, and R. B. Dunbar (2003), Decadal timescale shift in the ^{14}C record of a central equatorial Pacific coral, *Radiocarbon*, *45*, 91–99.

Gu, D., and S. G. H. Philander (1997), Interdecadal climate fluctuations that depend on exchanges between the tropics and the extratropics, *Science*, *275*, 805–807, doi:10.1126/science.275.5301. 805.

Guilderson, T. P., and D. P. Schrag (1998a), Radiocarbon variability in the western equatorial Pacific inferred from a high-resolution coral record from Nauru Island, *J. Geophys. Res.*, *103*, 24,641–24,650, doi:10.1029/98JC02271.

Guilderson, T. P., and D. Schrag (1998b), Abrupt shift in subsurface temperatures in the tropical Pacific associated with changes in El Nino, *Science*, *281*, 240–243, doi:10.1126/science.281.5374.240.

Guilderson, T. P., D. P. Schrag, E. Goddard, M. Kashgarian, G. M. Wellington, and B. K. Linsley (2000), Southwest subtropical Pacific surface water radiocarbon in a high-resolution coral record, *Radiocarbon*, *42*, 249–256.

Guilderson, T. P., D. P. Schrag, and M. A. Cane (2004), Surface water mixing in the Solomon Sea as documented by a high-resolution coral ^{14}C record, *J. Clim.*, *17*, 11471156, doi:10.1175/1520-0442(2004)017<1147:SWMITS>2.0.CO;2.

Hendy, E. J., M. K. Gagan, J. M. Lough, M. McColluch, and P. B. deMenocal (2007), Impact of skeletal dissolution and secondary aragonite on trace element and isotopic climate proxies in Porites corals, *Paleoceanography*, *22*, PA4101, doi:10.1029/2007PA001462.

Hughen, K. A., et al. (2004), Marine04 marine radiocarbon age calibration, 0–26 CAL KYR BP, *Radiocarbon*, *46*, 1059–1086.

Johnson, G., M. McPhaden, G. Rowe, and K. McTaggart (2000), Upper equatorial Pacific Ocean current and salinity variability during the 1996–1998 El Niño–La Niña cycle, *J. Geophys. Res.*, *105*(C1), 1037–1053, doi:10.1029/1999JC900280.

Konishi, K., T. Tanaka, and M. Sakanoue (1981), Secular variations of radiocarbon concentrations in seawater: Sclerochronological approach, in *Proceedings of the Fourth International Coral Reef Symposium*, vol. 1, pp. 181–185, ReefBase, Penang, Malaysia.

Marzaioli, F., G. Borriello, I. Passariello, C. Lubritto, N. De Cesare, A. D'Onofrio, and F. Terrasi (2008), Zinc reduction as an alternative method for AMS radiocarbon dating: Process optimization at CIRCE, *Radiocarbon*, *50*, 1–11.

Matsumoto, K., and R. M. Key (2004), Natural radiocarbon distribution in the deep ocean, in *Global Environmental Change in the Ocean and on Land*, edited by M. Shiyomi et al., pp. 45–58, TERRAPUB, Tokyo.

McGregor, H., and M. K. Gagan (2003), Diagenesis and geochemistry of *Porites* corals from Papua New Guinea: Implications for paleoclimate reconstruction, *Geochim. Cosmochim. Acta*, *67*(12), 2147–2156, doi:10.1016/S0016-7037(02)01050-5.

Müller, A., M. K. Gagan, and M. T. McCulloch (2001), Early marine diagenesis in corals and geochemical consequences for paleoceanographic reconstructions, *Geophys. Res. Lett.*, *28*(23), 4471–4474, doi:10.1029/2001GL013577.

Nydal, R., and K. Loveseth (1983), Tracing bomb ^{14}C in the atmosphere, *J. Geophys. Res.*, *88*, 3621–3642, doi:10.1029/JC088iC06p03621.

Picaut, J., and R. Tournier (1991), Monitoring 1979–1985 equatorial Pacific transports with expendable bathythermograph data, *J. Geophys. Res.*, *96*, Supplement, 3263–3277.

Reimer, P., et al. (2004), IntCal04 terrestrial radiocarbon age calibration, 0–26 cal kyr BP, *Radiocarbon*, *46*, 1029–1059.

Reverdin, G., C. Frankignoul, E. Kestenare, and M. J. McPhaden (1994), Seasonal variability in the surface currents of the equatorial Pacific, *J. Geophys. Res.*, *99*(C10), 20,323–20,344, doi:10.1029/94JC01477.

Rodgers, K. (2003), Extratropical sources of Equatorial Pacific upwelling in a OGCM, *Geophys. Res. Lett.*, *30*(2), 1084, doi:10.1029/2002GL016003.

Rubin, S. I., and R. M. Key (2002), Separating natural and bomb-produced radiocarbon in the ocean: The potential alkalinity method, *Global Biogeochem. Cycles*, *16*(4), 1105, doi:10.1029/2001GB001432.

Slota, P. J., A. J. T. Jull, T. W. Linick, and L. J. Toolin (1987), Preparation of small samples for ^{14}C accelerator targets by catalytic reduction of CO, *Radiocarbon*, *29*, 303–306.

Smith, T. M., R. W. Reynolds, T. C. Peterson, and J. Lawrimore (2007), Improvements to NOAA's historical merged land-ocean surface temperature analysis (1880–2006), *J. Clim.*, *20*(22), 5473–5496.

Southon, J., G. Santos, K. C. Druffel-Rodrigues, E. R. M. Druffel, S. Trumbore, X. Xu, S. Griffin, S. Ali, and M. Mazon (2004), The Keck carbon cycle AMS laboratory, University of California, Irvine: Initial operation and a background surprise, *Radiocarbon*, *46*, 41–49.

Stuiver, M., and H. A. Polach (1977), Discussion reporting of ^{14}C data, *Radiocarbon*, *19*, 355–363.

Taft, B. A., and W. S. Kessler (1991), Variations of zonal currents in the central tropical Pacific during 1970 to 1987: Sea level and dynamic height measurements, *J. Geophys. Res.*, *96*, 12,599–12,618, doi:10.1029/91JC00781.

Toggweiler, J. R., and S. Carson (1995), What are upwelling systems contributing to the ocean's carbon and nutrient budgets?, in *Upwelling in the Ocean: Modern Processes and Ancient Records*, pp. 337–360, John Wiley, New York.

Toggweiler, J. R., and K. Dixon (1991), The Peru upwelling and the ventilation of the South Pacific thermocline, *J. Geophys. Res.*, *96*(C11), 20,467–20,497, doi:10.1029/91JC02063.

Vogel, J. S., J. R. Southon, D. E. Nelson, and T. A. Brown (1984), Performance of catalytically condensed carbon for use in accelerator mass spectrometry, *Nucl. Instrum. Methods Phys. Res., Sect. B*, *5*, 289–293, doi:10.1016/0168-583X(84)90529-9.

Weisberg, R. H., and L. Qiao (2000), Equatorial upwelling in the central Pacific estimated from moored velocity profilers, *J. Phys. Oceanogr.*, *30*, 105–124, doi:10.1175/1520-0485(2000)030<0105:EUITCP>2.0.CO;2.

J. W. Beck, Physics and Geosciences Department, University of Arizona, Tucson, AZ 85721, USA.

C. D. Charles, Scripps Institution of Oceanography, University of California, San Diego, La Jolla, CA 92093, USA.

K. M. Cobb and H. R. Sayani, School of Earth and Atmospheric Sciences, Georgia Institute of Technology, Atlanta, GA 30332, USA.

E. R. M. Druffel and S. Griffin, Earth System Science Department, University of California, Irvine, CA 92697, USA.

R. G. Fairbanks, Earth and Planetary Science Department, Rutgers, State University of New Jersey, New Brunswick, NJ 08901, USA.

L. K. Zaunbrecher, Department of Geosciences, Georgia State University, 24 Peachtree Center Ave., Atlanta, GA 30303, USA. (lzaunbrecher1@student.gsu.edu)